Received February 2000
Revised October 2000
Accepted October 2000

Squish effect of piston crown on the turbulent heat transfer in reciprocating engine

Horng-Wen Wu and Shiang-Wuu Perng
Department of Naval Architecture and Marine Engineering, National Cheng Kung University, Tainan, Taiwan, Republic of China

Keywords *Engines, Heat transfer, Numerical analysis*

Abstract *An axisymmetric two-dimensional computer program employing the Large Eddy Simulation (LES) and SIMPLE-C method coupled with preconditioned conjugate gradient methods is applied to the turbulent flows in the compression-expansion strokes for various combustion chamber geometries under realistic engine conditions. The squish area percent of piston crown is changed (SQ = 0 percent for flat piston model, SQ = 46 percent for shallow bowl piston model and SQ = 76 percent for deep bowl piston model) under engine speeds (500~1,500rpm) for the purpose of investigating the heat transfer performance. Comparison was made of present heat flux results and earlier experimental and numerical results. It is shown that the numerical method can predict the turbulence with reasonable accuracy. The results show that the configuration of piston crown for squish area percent can obviously enlarge the surface heat flux of wall boundaries in reciprocating engines.*

Nomenclature

A = area of wall boundary surface
B = engine bore
BDC = bottom dead center
C_P = specific heat at constant pressure
CR = compression ratio
h = heat transfer coefficient
K = coefficient of thermal conductivity
K_{eff} = effective coefficient of thermal conductivity ($K_{eff} = K + \frac{C_P \rho \nu_T}{Pr_T}$)
L = mixing length
L_{ref} = reference lengths
$L_{head\text{-}piston}$ = distance from cylinder head to piston
L_s = engine stroke
L_r = connecting rod length
N = engine speed (rpm)
P = pressure
Pr_T = turbulent Prandtl number ($Pr_T = 0.9$)
q_w = wall heat flux
$\overline{q_w}$ = mean surface heat flux ($\frac{\int q_w dA}{\int dA}$)
R = gas constant
S_Φ = source term for variable
SR = initial swirl ratio ((initial swirl velocity)/(2 $\pi r \times$ RS))
SQ = squish area percent ($\left(\frac{\text{piston-top area excluding bowl}}{\text{cylinder cross-sectional area}}\right) \times 100\%$)
t = time
T = temperature
T_w = wall temperature
TDC = top dead center
u = velocity component parallel to the wall
u_* = friction velocity
U_x, U_r, U_θ = velocity components along x , r and θ axes
$\overline{U}$ = velocity vector
ω = vorticity ($\frac{\partial U_x}{\partial r} - \frac{\partial U_r}{\partial x}$)
x_i = coordinates (i = 1 for axial coordinate x; i = 2 for radial coordinate r)
X_w = normal distance from the wall
y = distance from the wall
y_* = dimensionless distance from the wall

International Journal of Numerical Methods for Heat & Fluid Flow, Vol. 11 No. 1, 2001, pp. 76-97.

The authors gratefully acknowledge the partially financial support of this project by the National Council of the Republic of China.

Greek letters

α = constant equal to 0.2
Δ = filter width
κ = Von Karman constant
Γ_Φ = diffusion coefficient
μ = laminar dynamic viscosity
μ_{eff} = effective dynamic viscosity ($\mu_{\text{eff}} = \mu + \rho\nu_T$)
ν = molecular kinematic viscosity
ν_T = turbulent kinematic viscosity
ρ = density
Φ = general dependent variable
τ_w = wall shear stress
θ = crank angle (degrees)

Introduction

The wall heat transfer and fluid dynamics occurring in reciprocating internal combustion engines play an important role for engine design, engine performance improvement, and mixing of air and fuels. Hence, the ability to predict the magnitude of the heat transfer between the working fluid and combustion chamber walls is very important to the designer. There are many parameters that affect wall heat flux of an engine, such as engine speed, load, material, chemical reaction, initial swirl ratio, compression ratio, turbulent transport, and geometry of the combustion chamber (Dao *et al.*, 1973; Morel *et al.*, 1987; Woschni and Fieger, 1980; Yamada *et al.*, 1989; Assanis and Badillo, 1989).

Several studies have been conducted on the geometry of a combustion chamber to determine fluid flow using numerical methods. Gosman *et al.* (1984) reported the 3-D air flow in the engine by utilizing the $k - \varepsilon$ model, but he emphasized the phenomenon of the fluid and did not investigate the influence of all parameters on the fluid field. Kondoh *et al.* (1986) used 2-D axisymmetric turbulent model to study the influence of the shape of the combustion chamber on the appearance of fluid flow. Ikegami *et al.* (1986) presented the numerical heat transfer results in the 2-D axisymmetric turbulent model engine by utilizing the SIMPLE scheme, but the influence of the configuration of the combustion chamber on the surface heat transfer was not involved. The previous numerical literature has been conducted on the form of the combustion chamber influence on fluid flow, but few investigated the influence on wall heat transfer. The purpose of this paper is to numerically quantify the influence of squish area percent of the piston crown on heat transfer at various crank angles by changing engine speed.

The Reynolds-averaged simulations require a fine grid to resolve the regions of rapid variations. Given the complexity of the Reynolds-averaged simulations, a Large Eddy Simulation (LES) might actually be simpler, shorter in execution and more accurate. In the Reynolds-averaged simulations the length scales of the turbulence usually are much larger than the grid spacing. The Reynolds-average simulations only reveal unsteady motions of scales larger than the model's turbulence scale. Besides, the eddy viscosity is obtained from the length scale of the smallest eddy in the turbulent models. Therefore, the volume-average filtered Navier-Stokes equations are fairly insensitive to the turbulent models in a Large Eddy Simulation (LES) (Fureby *et al.*, 1997).

This paper utilizes a SIMPLE-C method of Raithby and Van Doormaal (1984) and Large Eddy Simulation (Galperin and Orszag, 1993) (LES) to investigate the turbulent flow modification by means of vortex and squish appearances generated by squish area percent and their effect on heat transfer along the wall surfaces. Extended Linear Upwind Differencing (ELUD) method (Tsui, 1991) (third-order scheme) is implemented for discretizing the convection terms to avoid several oscillations. Also, iterative solution methods based on the preconditioned conjugate gradient method, including Incomplete Cholesky Conjugate Gradient (Kershaw, 1978) (ICCG) method for symmetric matrices and Incomplete LU Bi-Conjugate Gradient (Van Der Vorst, 1992) (ILUBiCG) method for nonsymmetric matrices, were incorporated into the solving process with second-order time advancement. Time-independent grid system (Tu and Fuchs, 1992), in which completely new grids are not necessarily generated at each time step, for mesh generation is used here for constructing a local computational region attached to the moving boundary (moving piston). It generally requires much less computer storage and computation time than the conventional method with the single-grid at various crank angles. The results of this study may be of interest to engineers attempting to develop thermal control of engine configurations and to researchers interested in the flow-modification aspects of heat transfer in the combustion chamber.

Mathematical model

Calculation of the reciprocating thermal flow field in a motored engine requires obtaining the solution of the governing equations. The transport equations representing the conservation of mass, momentum, and thermal energy are cast into a general form of time-dependent and axisymmetric cylindrical coordinates:

$$\frac{\partial(\rho\Phi)}{\partial t}+\frac{1}{r}\left[\frac{\partial}{\partial x}(\rho U_x r\Phi)+\frac{\partial}{\partial r}(\rho U_r r\Phi\right] = \frac{1}{r}\left[\frac{\partial}{\partial x}\left(r\Gamma_\Phi\frac{\partial\Phi}{\partial x}\right)+\frac{\partial}{\partial r}\left(r\Gamma_\Phi\frac{\partial\Phi}{\partial r}\right)\right]+S_\Phi(x,r) \tag{1}$$

where Φ represents one of the following entities: 1, U_x, U_r, U_θ, or T, in which the dependent variables are axial velocity U_x, radial velocity U_r, swirl velocity U_θ, and temperature T. Also, t is time, ρ denotes density, and Γ_Φ and S_Φ stand for the corresponding effective diffusion and source term, respectively. The corresponding expressions of Γ_Φ and S_Φ are given in Table I. In Equation (1), the notation $\Phi = 1$ denotes the continuity equation.

In Table I, μ is the molecular viscosity and can be calculated by the Sutherland law, μ_{eff} is the effective viscosity, P is pressure, R is the gas constant, K_{eff} is the effective coefficient of thermal conductivity, K is the coefficient of thermal conductivity, and C_P is the specific heat at constant pressure. Assume the fluid to be an ideal gas with constant C_P, then simplifying

Φ	Γ_Φ	S_Φ
1	0	0
U_x	μ_{eff}	$-\frac{\partial P}{\partial x}+\frac{\partial}{\partial x}\left(\mu_{eff}\frac{\partial U_x}{\partial x}\right)+\frac{\partial}{r\partial r}\left(r\mu_{eff}\frac{\partial U_r}{\partial x}\right)+\frac{\partial}{\partial x}\left(\mu_{eff}\nabla\cdot\overline{U}\right)$
U_r	μ_{eff}	$-\frac{\partial P}{\partial r}+\frac{\partial}{\partial x}\left(\mu_{eff}\frac{\partial U_x}{\partial r}\right)+\frac{\partial}{r\partial r}\left(r\mu_{eff}\frac{\partial U_r}{\partial r}\right)+\frac{\rho U_\theta^2 z}{r}-2\frac{\mu_{eff}U_r}{r^2}+\frac{\partial}{\partial r}\left(\mu_{eff}\nabla\cdot\overline{U}\right)$
U_θ	μ_{eff}	$-\rho\frac{U_\theta U_r}{r}-\frac{\partial}{r\partial r}\left(r\mu_{eff}\frac{U_\theta}{r}\right)+\mu_{eff}\frac{\partial\left(\frac{U_\theta}{r}\right)}{\partial r}$
T	$\frac{K_{eff}}{(C_P-R)}$	0

Note: $\mu_{eff}=\mu+\rho\nu_T$, $K_{eff}=K+\frac{C_P\rho\nu_T}{Pr_T}$ $(Pr_T=0.9)$

Table I.
Definition of Φ, Γ_Φ and S_Φ

the energy equation by neglecting internal heat generation, dissipation, radiation heat flux, and energy source (Smith, 1996).

Turbulence modeling

On initial runs of the present research it was discovered that the Smagorinsky model (Smagorinsky, 1963) did not generate sufficient levels of eddy viscosity. The form of Baldwin-Lomax model (Wilcox, 1993) is similar to the Smagorinsky model and is as follows: $\nu_T = L^2|\omega|$, where $|\omega|$ is the magnitude of the vorticity. L is the mixing length independent of the grid size. The mixing length was chosen as the minimum of all of the mixing lengths calculated to ensure smooth transitions.

$$L=\min\left(\kappa X_w, \alpha\frac{B}{2}, \alpha L_{head-piston}\right) \tag{2}$$

where X_w is normal distance from the wall, B is engine bore and $L_{head\text{-}piston}$ is distance from cylinder head to piston.

Boundary conditions

Flow and temperature fields in the near-wall regions are matched to the boundary layer models. The wall function (Amsden *et al.*, 1985) is used to provide wall boundary conditions for velocity and temperature, respectively.

In the laminar sublayer (when $y_* < 130.3$),

$$\frac{u}{u_*} = \sqrt{y_*} \tag{3}$$

$$h = \frac{1.125\rho\nu C_P}{y} \tag{4}$$

$$q_w = h(T - T_w) \tag{5}$$

In the turbulent boundary layer (when $y_* \geqq 130.3$),

$$\frac{u}{u_*} = 0.75 + 2.19 \ln y_* \tag{6}$$

$$h = 1.125\left(\frac{\tau_w}{u}\right)C_P \tag{7}$$

$$q_w = h(T - T_w) \tag{8}$$

where $y_* \equiv \rho|u|y/\mu$, u is the velocity component parallel to the wall, u_* is the friction velocity, y is the distance from the wall, h is the heat transfer coefficient, T_w is the wall temperature, ν is the molecular kinematic viscosity, the wall shear stress $\tau_w = \rho u_*|u_*|$, and q_w is the heat flux to the wall.

No-slip boundary conditions are applied for velocities at all walls. At the piston crown, the axial velocity U_x is assumed to equal the moving velocity of the piston. The wall temperature is assumed to be 350K, thereby simulating the case of a cold engine state.

Initial conditions

Each calculation starts at a crank angle of 240° (120° BTDC) and terminates at 390° (60° ATDC) for various engine speeds. The initial air condition is assumed to be a solid-body rotation profile, $U_\theta(r) = 2\pi N \cdot SR \cdot r$, where N is the engine speed and SR (called the swirl ratio) is defined as the ratio of swirling speed (rpm) of the gas to engine speed. The initial swirl ratio is 2.15. The axial velocity U_x is assumed to vary linearly from cylinder head surface (zero velocity) to piston crown surface (moving boundary velocity). The radial velocity U_r is assumed to be zero. The initial temperature is set equal to be 350K. The engine used for computation is a four-stroke engine with various bowl model pistons. The main specifications of the engine are illustrated in Figure 1(a).

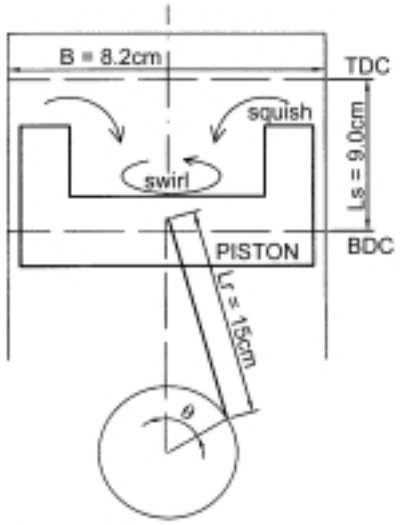

(a) Engine geometry used here

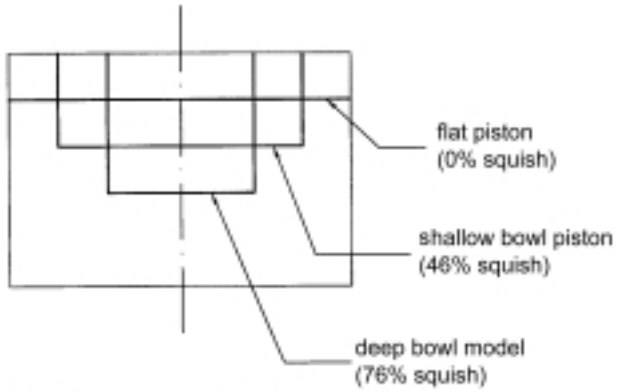

(b) Squish area percent for three models

Figure 1.
(a) Engine geometry used; (b) squish area percent for three models

Numerical method

Formulation and discretization of all transport equations are performed by using the SIMPLE-C algorithm with the control volume approach, with each equation arranged into transient, diffusion, convection, and source terms.

Convective term

In this phase, extended linear upwind differencing (ELUD) is utilized to discretize the convective terms of governing equation. ELUD is the third-order accurate upwinding scheme.

Time advancement

Due to the fact that second-order backward Euler (SBE) would be easy to implement in a SIMPLE-C Navier-Stokes solver, this scheme is chosen for this work.

$$\frac{\partial \Phi_i}{\partial_t} = \frac{\frac{3}{2}\Phi_i^{n+1} - \frac{4}{2}\Phi_i^{n} + \frac{1}{2}\Phi_i^{n-1}}{\Delta t} \tag{9}$$

Iterative method

Iterative solution methods based on the preconditioned conjugate gradient method are incorporated into this code and evaluated. In this study, the ICCG method is used for Poisson pressure correction equation, and the ILUBiCG method is used for U_x, U_r, U_θ, T equations. The crank angle step was set as 1° for the calculations of unsteady flow and heat transfer in the cylinder chamber; we consider the difference of the calculated velocity fields and the mass residual as convergence conditions. The calculations were terminated when the mass residual is less than 10^{-4} and the solution of velocity varied less than 10^{-5}.

Grid generation approach

In this study, the approach is used to treat the moving piston as a moving solid body in the computational domain without generating completely new grids at each time step. When the piston moves toward TDC or from TDC, the size of the domain will vary with the motion of the piston and those grids lying outside the body will be flagged as unused points which are excluded from the calculation. When the piston was moving away from TDC it was necessary not only to interpolate the values back to their fixed grid locations, but also extrapolate the values of the time dependent variables for two grid cells into the piston. This extrapolation was performed with a second-order Lagrange polynomial.

Results and discussion

A detailed numerical study has been carried out on the turbulent heat transfer in the internal flow field of the motored engine. The walls of the cylinder chamber, including cylinder head surface, piston crown surface, and cylinder wall surface are shown in Figure 1(a).

In this study, the engine speed (N) is taken as 500, 1,000 and 1,500rpm when the initial swirl SR is 2.15. Three types of piston crown are considered as Figure 1(b) shows. The first has no bowl in the piston crown and is called a "flat piston model" (SQ = 0 percent). The other two have a bowl in the piston crown and are called either "shallow bowl piston model" (SQ = 46 percent) or "deep bowl piston model" (SQ = 76 percent) depending on the depth of the bowl as compression ratio is kept at 9.5. All the calculations have been performed by using a PENTIUM 200 PC. After a series of test runs, a SIMPLE-C mesh (grid

32 × 63 for 240° (120° BTDC)~ grid 32 × 20 for 360° (TDC)~ grid 32 × 25 for 390° (30° ATDC)) was chosen for all cases. Further refinement changed the values of local heat flux less than 0.05 percent for the test runs. The calculation for the flat piston model utilized 150 angle steps and the computation time was about 1h 3min 35s of CPU time. The other two cases were about 1h 36min 17s and 1h 31min 42s of CPU time.

To show that the program in this study can handle turbulent heat transfer in a motored engine correctly, we apply the present method to solve the unsteady heat transfer in a motored engine with a flat piston crown employed by Yang *et al.* (1988). The engine parameters used by them and us include bore (91.9mm), stroke (76.2mm), compression ratio (CR = 9.5) and initial swirl ratio (SR = 0.5) while the engine speed is 750rpm and 1,446rpm. The predicted transient heat flux on head surface presented in Figure 2 agrees well with the experimental data and calculated results of Yang *et al.* (1988).

In this study, the mean surface heat flux for cylinder head, cylinder wall and piston crown is thereafter used for comparing the heat transfer characteristics among three types of piston crown. The mean surface heat flux on the surface is presented in Figure 3 for different parts of deep bowl piston model and different crank angles, ranging from 300° (60° BTDC) to 390° (30° ATDC), at 1,000rpm. For cylinder head surface, the peak value

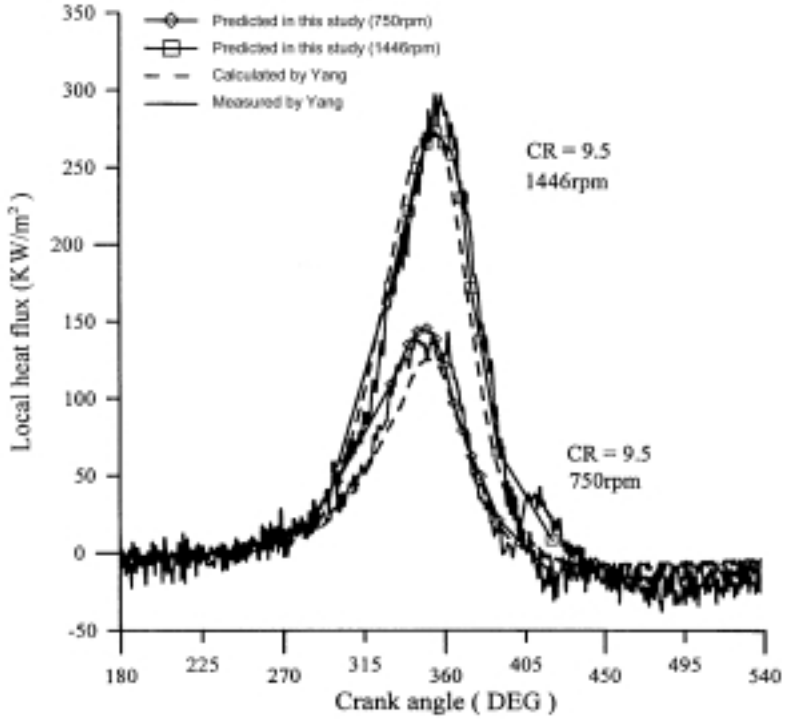

Figure 2.
Comparison of predicted local wall heat flux on cylinder head surface with experimental data and calculated results pf Yang (r = 20.0mm)

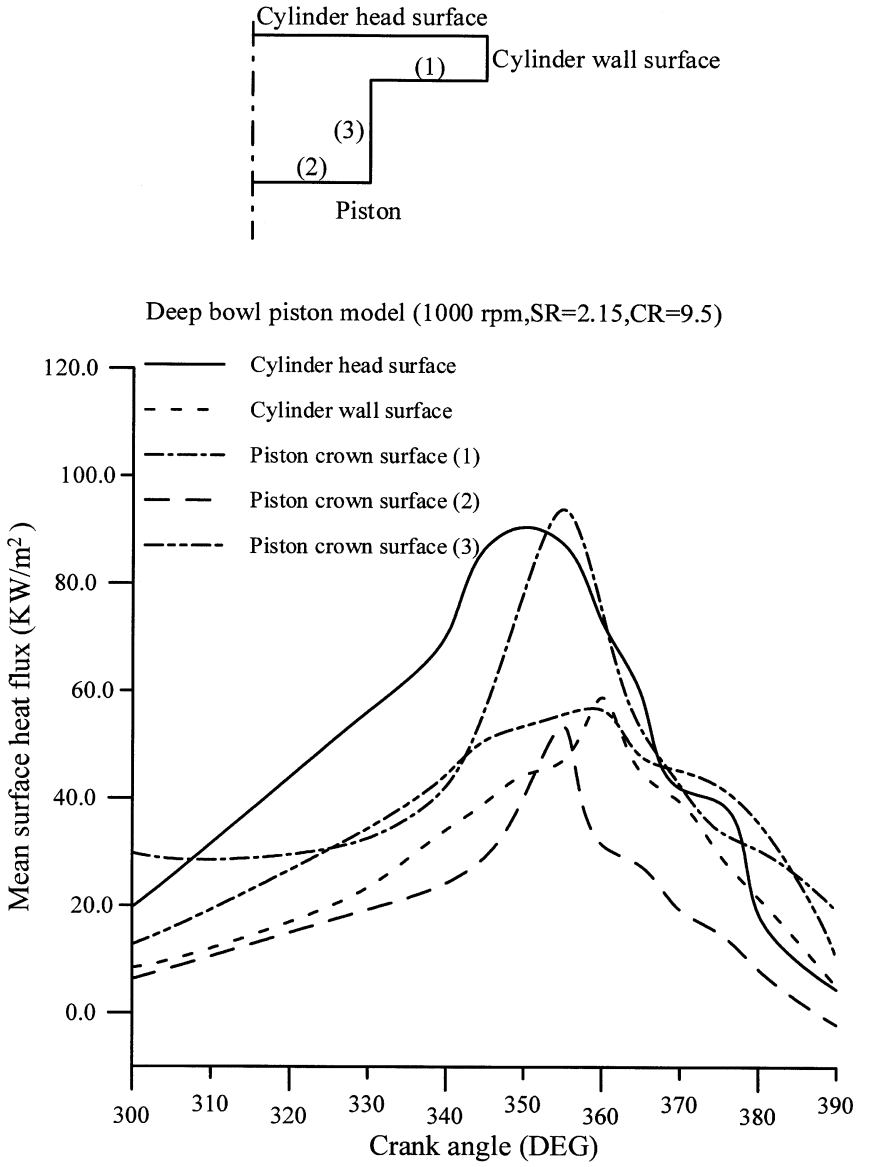

Figure 3.
Transient mean surface heat flux on different surfaces for various crank angles in deep bowl piston model

occurs at 350° (10° BTDC); 355° (5° BTDC) for piston crown surface (1) and (2); 360° (TDC) for piston crown surface (3) and cylinder wall surface. Besides, it may be noted that the surface heat fluxes near 5° BTDC are much higher for cylinder head surface and piston crown surface (1) than for the cylinder wall and the other two piston crown surfaces. This behavior implies that there is an obvious squish effect on cylinder head surface and piston crown surface (1) from crank angles 350° to 360°. For cylinder head, the deep bowl piston

model has higher local heat fluxes on region II than on region I and the shallow bowl piston model also has higher ones on region B than on region A at crank angle 350° as shown in Figure 4. The result presents regions II and B to be influenced by squish motion. Similar observations have been seen in an earlier experimental study (Morel *et al.*, 1987). The combined velocity vectors of U_x and U_r at 300° (60° BTDC), 330° (30° BTDC), 350° (10° BTDC), 360° (TDC), 370° (10° ATDC), and 390° (30° ATDC) are presented in Figure 5 to explain the results of Figure 3. At 300°, an increase in upward piston speed causes radial velocity vectors much smaller than axial ones near the piston crown (Figure 5(a)). This causes mean surface heat fluxes on all small surfaces (Figure 3). When the piston continues to compress upward until

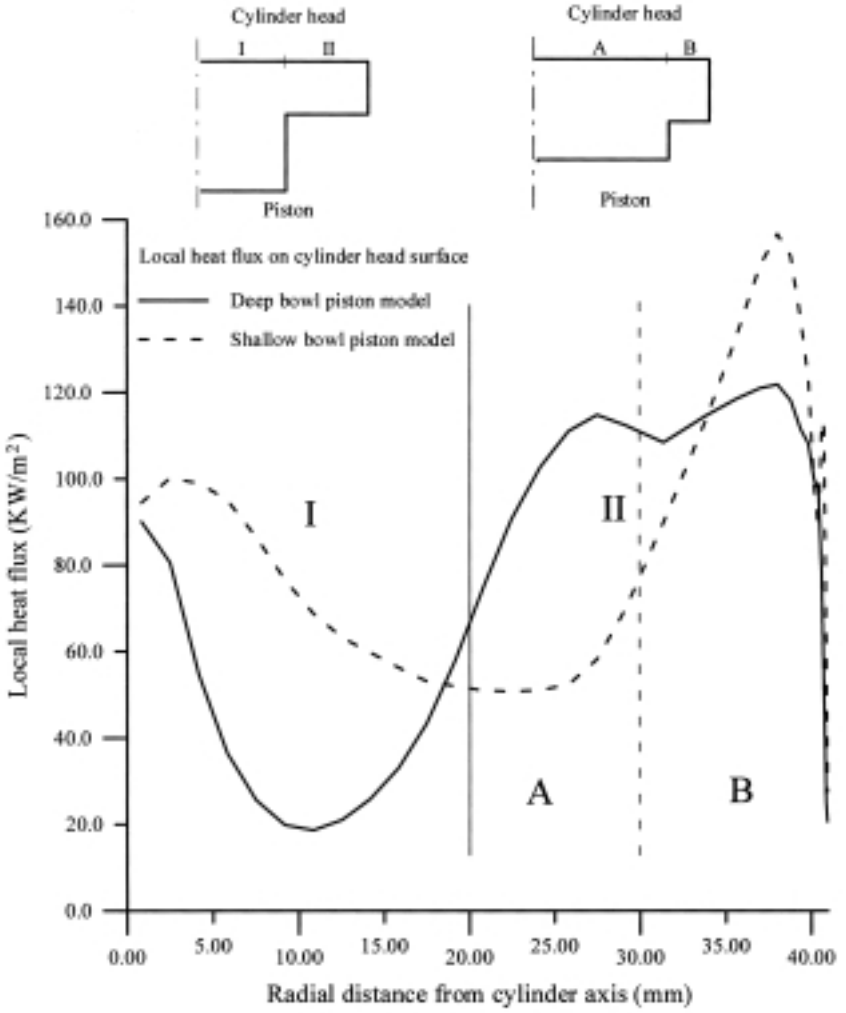

Figure 4.
Local wall heat flux on cylinder head surface for deep and shallow bowl piston models (θ = 350°)

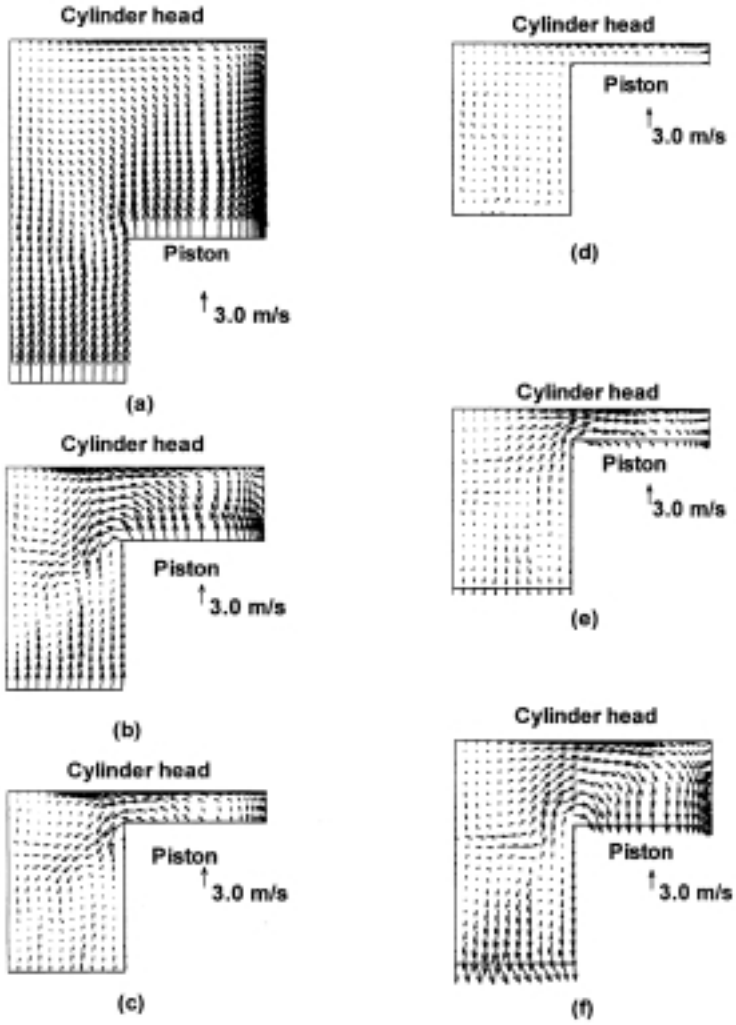

Note: The combined velocity vectors of U_x and U_r for deep bowl piston model at θ equal to (a) 300°; (b) 330°; (c) 350°; (d) TDC; (e) 370°; (f) 390°

Figure 5.

330°, the instantaneous piston speed is weaker and the squish effect is going to develop after the fluids are brought from the periphery into the piston bowl (Figure 5(b)). Moreover the squish motion interacting with higher swirl velocity can form the vortex in the bowl. At this time, the mean surface heat flux is higher for cylinder head than for the other parts (Figure 3). At 350°, the stronger squish effect with weaker piston speed produced an obvious vortex in the bowl and a slight one in the left region around cylinder head (Figure 5(c)). This effect also strengthens the mean surface heat flux much more for

cylinder head surface and piston crown surface (1) than for the other parts (Figure 3). At TDC the squish motion almost terminates (Figure 5(d)), so the higher two heat fluxes reduce suddenly (Figure 3). After the piston passes through TDC, owing to downward piston motion, the fluids are sucked up into the periphery, and the appearance forms the reversed squish motion. At 370° the reversed squish produces a slight vortex opposite to one at 350° in the bowl (Figure 5(e)). About 390°, due to weaker reversed squish and swirl velocity, the vortex in the bowl will vanish gradually (Figure 5(f)). At that moment, the heat fluxes are minimum and tend to be negative; that is, the heat is going to transfer from walls to the fluids (Figure 3). These results can provide confirmation to the heat transfer and flow processes in an engine cylinder.

Increasing the squish area percent of piston crown increases the mean surface heat fluxes on different parts (piston crown surface including piston crowns (1), (2), and (3)) for three piston models at 1,000rpm as shown in Figure 6. The peak values are obviously higher for shallow (SQ = 46 percent) and deep (SQ = 76 percent) bowl models than for flat (SQ = 0 percent) model. Before 340° the heat fluxes are slightly lower for deep model than for shallow model as shown in Figure 6(a). At 300° (60° BTDC), due to having no squish motion yet, the phenomenon of flow field is similar along the surface of the cylinder head and cylinder wall for three piston models. For both bowl piston models, crown surface (3) has flow velocity parallel along it but crown surfaces (1) and (2) do not have (see Figure 5(a)), so the phenomenon of heat transfer is different from the flat piston model. Summing up the above statement for 300° (60° BTDC), the mean surface heat flux is approximately the same for three models in Figure 6(a) and (b), but it differs significantly in Figure 6(c). For both bowl piston models, during expansion the inverse squish motion is suddenly becomes stronger at 370° (10° ATDC) around the cylinder head (as shown in Figure 5(e)), and the sudden change then causes the humps in the heat transfer at approximately 370°. The peak values of heat flux occur between 350° (10° BTDC) and 360° (TDC), also shown in Figure 6. Similar expressions have been seen in a previous study conducted by Lawton (1987) in which the maximum heat flux occurred about 8° before TDC. This can be explained by his findings that during compression the heat flux is small until the timing at which gas pressure starts to rise steeply. Besides, the differences in the squish intensity only change the magnitude of temperature gradient but the timing of a steep rise in pressure is common. As a result, the timing for the mean surface flux to show a peak is common for three models in Figure 6(a) and (c) (both surfaces normal to the direction of piston motion) despite the differences in the squish intensity. In order to realize the relation of heat transfer and squish effects, we can observe the fluids flow at 350° and 355°, and the isothermal plots at 350°, TDC and 370° for three models in Figures 7, 8 and 9. In Figure 7(a), the fluid for the flat piston model cannot produce squish motion, so the fluid velocity vectors along all the surfaces are slower and weaker from a comparison with shallow and deep bowl models.

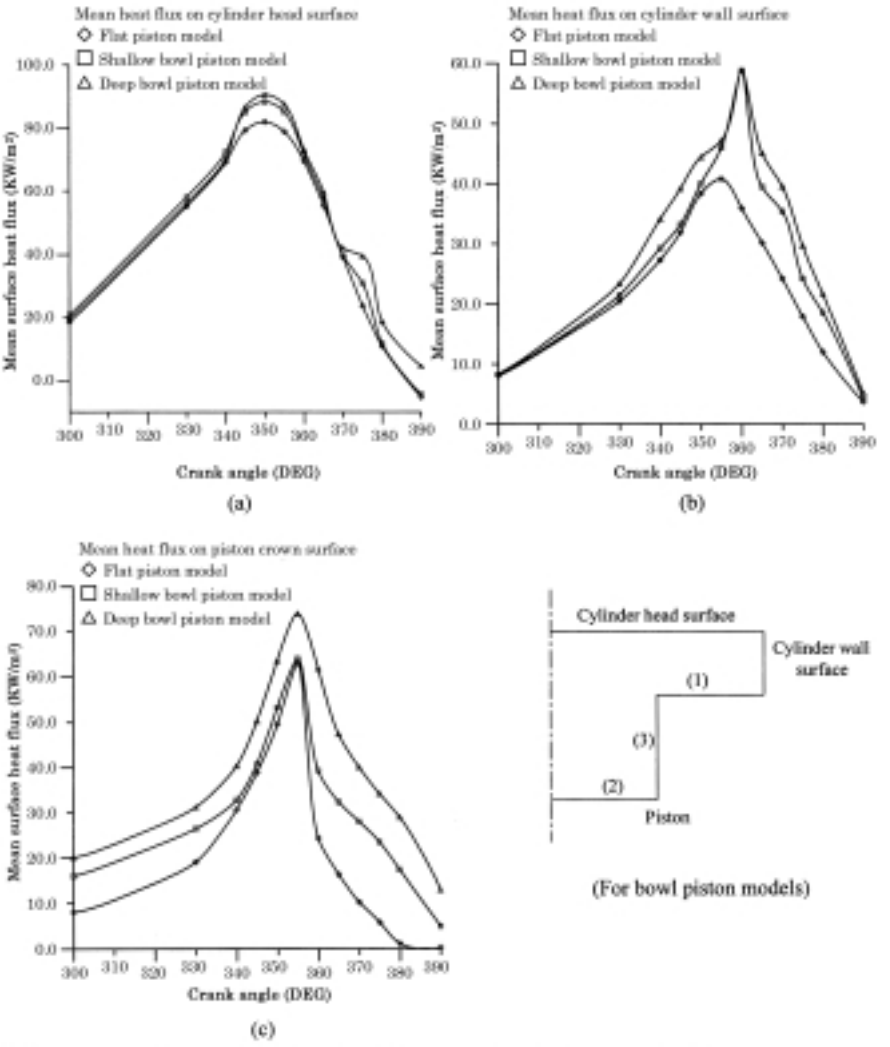

Note: Transient mean surface heat flux at different crank angles on (a) cylinder head surface; (b) cylinder wall surface; (c) piston crown surface for three models

Figure 6.

Furthermore, the mean surface heat fluxes at various walls for the flat piston are the minimum values in three models. Besides, there seems to be a weak vortex in the right region around the cylinder wall; but the vortex is not caused by squish effect, it is formed since the upward fluid flow hits the cylinder head. In Figure 7(b), the size of squish area is not enough to produce a vortex in the bowl, and the squish motion destroys the vortex existing in the flat piston model. In the deep bowl piston model (Figure 7(c)), the strong

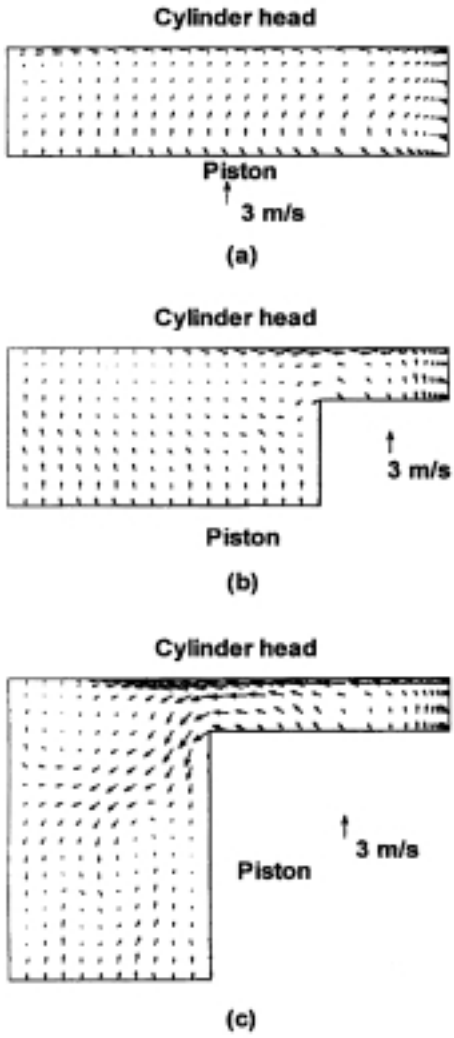

Note: The combined velocity vectors of U_x and U_r at crank angle 350° for (a) flat piston model; (b) shallow bowl piston model; (c) deep bowl piston model (1,000rpm)

Figure 7.

squish effect is enough to form a vortex in the bowl and a secondary vortex in the left region around the cylinder head. The secondary vortex rotates in the direction opposite to that of the vortex in the bowl. The trends of Figure 8 in flow structure for the three models are the same as those of Figure 7, but the piston speed is smaller for 355° than for 350° and all vortexes and squish motions are weaker. Figure 9 illustrates the isothermal distribution of the

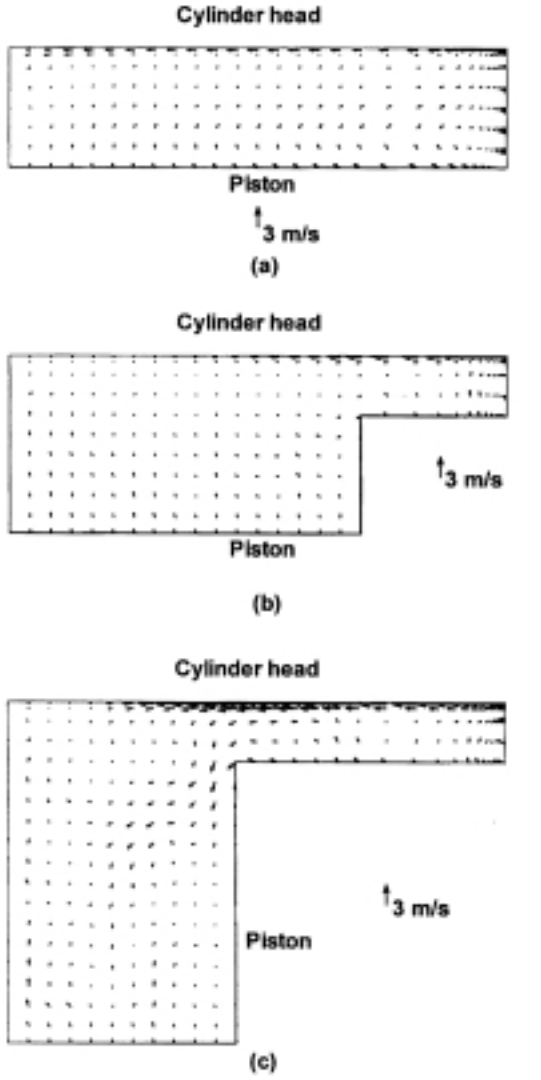

Note: The combined velocity vectors of U_X and U_Y at crank angle 355° for (a) flat piston model; (b) shallow bowl piston model; (c) deep bowl piston model (1,000rpm)

Figure 8.

three piston models for the different crank angles. Closer isothermal lines indicate a higher temperature gradient and accordingly a higher heat flux. The parallel velocity and the temperature gradient along the region II of cylinder head (see Figure 4) in the deep bowl piston model is the maximum among the three models, hence the deep bowl piston has the strongest radial

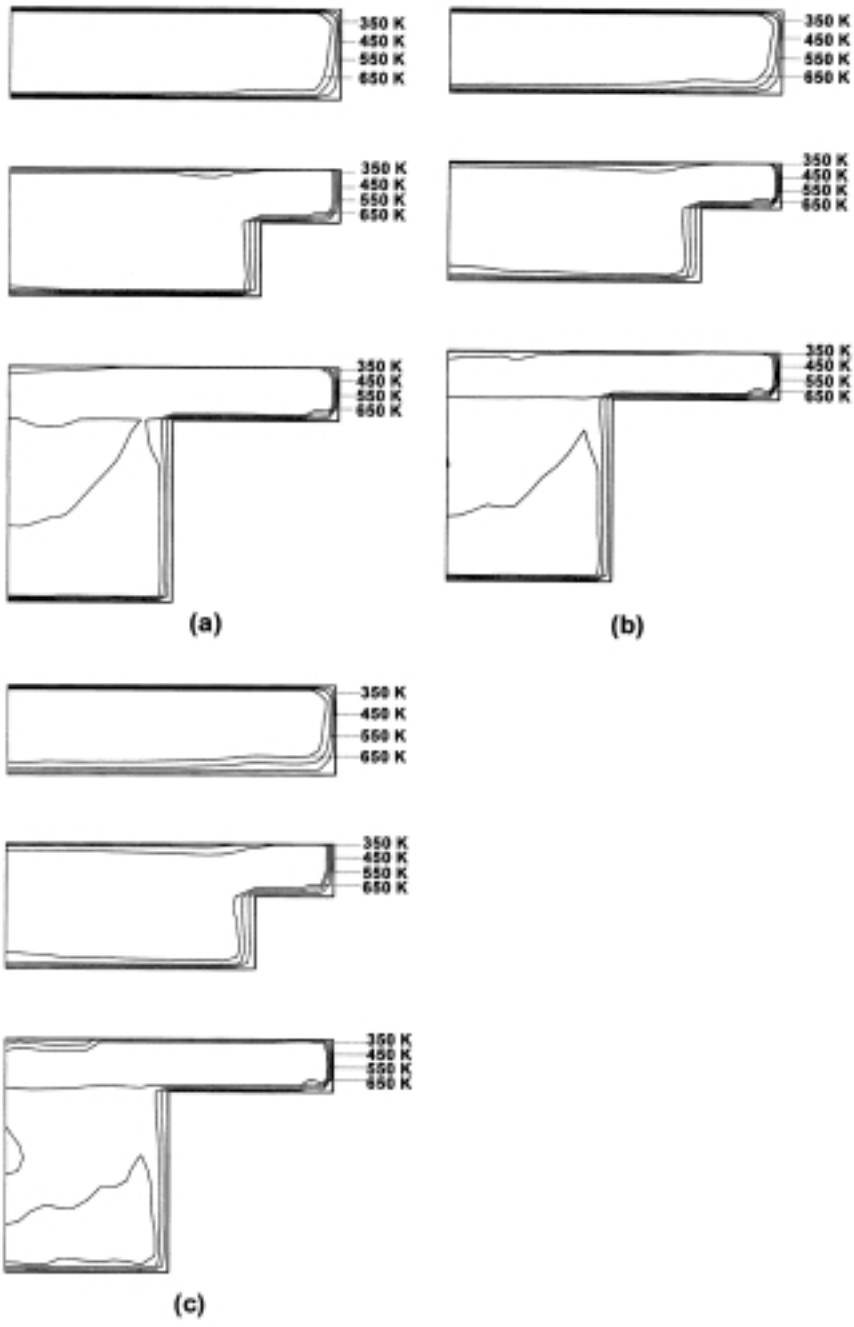

Note: Isotherms for various piston models at (a) 350°; (b) TDC; (c) 370°

Figure 9.

velocity and the largest heat flux along the cylinder head. For the cylinder wall, the parallel velocity and the temperature gradient along the surface become larger due to the squish motion, and therefore the mean heat flux in the deep bowl piston model is the maximum. There is a vortex in the bowl of the piston for the deep bowl piston model to cause a smaller gas mean-temperature in the bowl of the piston than for the other two models. In addition, the temperature gradient along the region of piston opposite region II of the cylinder head is large also due to squish effect. Therefore, the surface mean heat flux of the piston for the deep bowl piston model is the maximum among the three models. The isothermal plots in Figure 9 can be used to explain the timing for the peak of mean heat flux as shown in Figure 6. For example, the temperature gradient along cylinder head at 350° is the largest among three crank angles. Then it has the largest values of mean heat flux as shown in Figure 6(a)

The mean value of surface heat fluxes increases with increasing engine speed, and the increase quantity near the peak value of heat flux is much larger, especially on the cylinder head and cylinder wall surface (Figures 10(a) and (b)). We may investigate the above results by observing the velocity vectors plots and the isothermal plots in Figures 11 and 12. All fluid motions become stronger as the engine speed increases. This increases squish strength and the temperature gradient along the surface of each part in the engine, so the heat fluxes on the surfaces increase obviously. Besides, we can find that the local high temperature in the bowl is becoming larger as the engine speed increases. Moreover, the peak value of heat flux increases much larger due to larger squish effect.

We may investigate the influence of squish area percent of the piston crown on heat transfer by means of the values of mean surface heat flux for the boundary surfaces. The value of mean surface heat flux for all the surface increases with increasing squish area percent for the three models at various N values. The maximum value of mean heat flux occurs at the cylinder head, while the minimum value occurs at the cylinder wall with obvious squish effect (between 340° and TDC). For 1,500rpm in the deep bowl piston, the maximum value of mean surface heat flux occurs at 355° through compression stroke while that value occurs at 365° through expansion stroke. The maximum increase in overall mean surface heat flux is 60 percent when the crank angle is 360° (TDC) with 500rpm for the deep bowl piston model through compression stroke. Besides, it is about 65.5 times when the crank angle is 390° with 1,500rpm for deep bowl piston model through expansion stroke. The increase in the overall mean surface heat flux on the piston crown surface is much larger than on the other two surfaces. This result is primarily contributed by an increase in the mean surface heat flux with various crank angles, piston models, and N values, because the squish area percent enlarges the heat transfer on the piston crown surfaces.

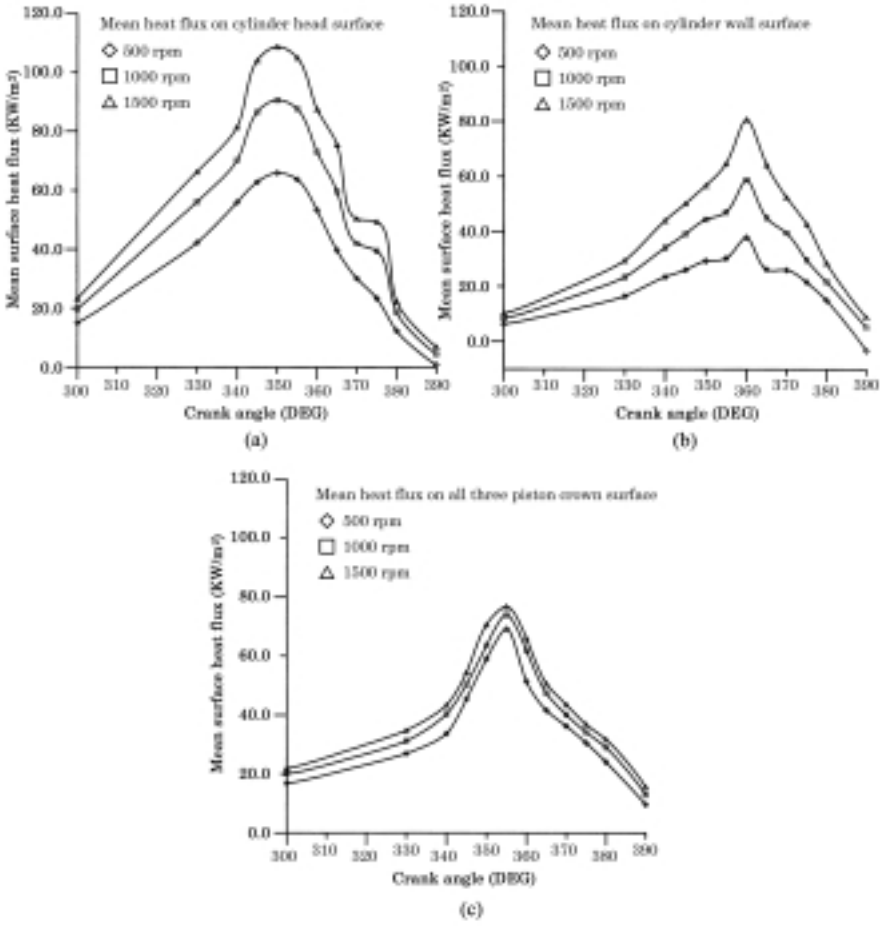

Note: Transient mean surface heat flux at different N on (a) cylinder head surface; (b) cylinder wall surface; (c) piston crown surface in deep bowl piston model

Figure 10.

Conclusions

Numerical investigation has been systematically performed on the unsteady flow and turbulent heat transfer in reciprocating engines with and without considering the squish area on the piston crown. On the basis of these results presented and discussed in the discussion section, we draw the main conclusions below:

- Coupling the piston axial velocity and squish effect has profound influences in determining the unsteady flow fields and heat transfer characteristics.
- The squish effect exists obviously along the surfaces of wall boundaries between 340° (20° BTDC) and 360° (TDC), hence the maximum mean surface heat flux occurs between 350° (10° BTDC) and 360° (TDC).

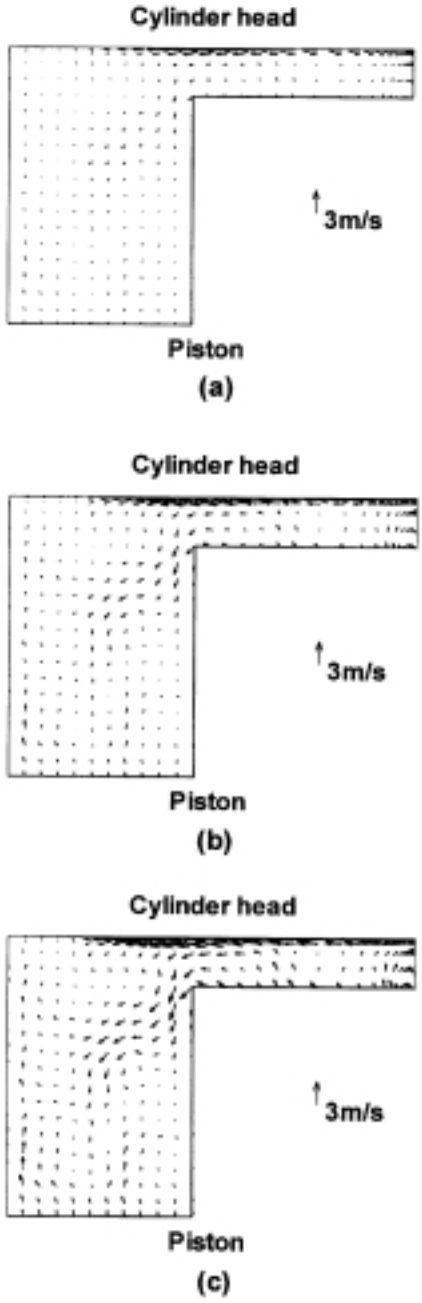

Note: The combined velocity vectors of U_x and U_r at $\theta = 355°$ in deep bowl piston model for (a) 500rpm; (b) 1,000rpm; (c) 1,500rpm

Figure 11.

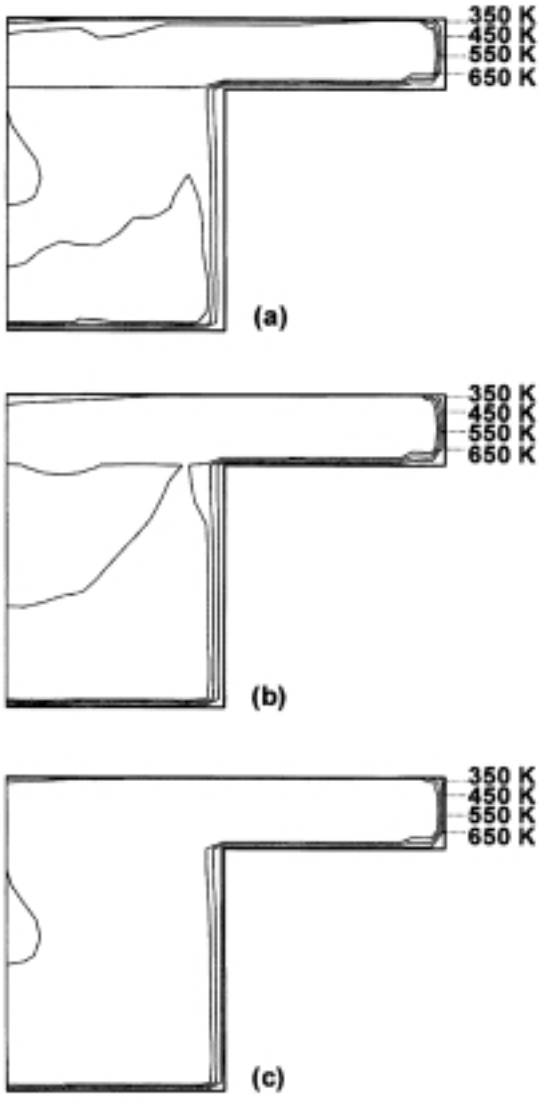

Note: Isotherm at θ = 355° in deep bowl piston model for (a) 500rpm; (b) 1,000rpm; (c) 1,500rpm

Figure 12.

- Increasing the squish area percent of the piston crown will increase the strength of the induced squish flow and the wall heat flux.
- For three different models at various values of engine speed, the maximum increase in overall mean surface heat flux is 60 percent when

the crank angle is 360° (TDC) for deep bowl piston model through compression stroke with 500rpm. Through expansion stroke, the maximum value is 65.5 times when the crank angle is 390° (30° ATDC) for the same model with 1,500rpm.

References

Amsden, A.A., Ramshaw, J.D., O'Rourke, P.J. and Dukowicz, J.K. (1985), "KIVA: a computer program for two- and three-dimensional fluid flows with chemical reactions and fuel sprays", *Los Alamos National Lab. Report, LA-10245-MS*, Los Alamos, CA.

Assanis, D.N. and Badillo, E. (1989), *Evaluation of Alternative Thermocouple Designs for Transient Heat Transfer Measurements in Metal and Ceramic Engines*, SAE 890571.

Dao, K., Uyehara, O.A. and Myers, P.S. (1973), *Heat Transfer Rates at Gas-Wall Interfaces in Motored Piston Engine*, SAE 730632.

Fureby, C., Tabor, G., Weller, H.G. and Gosman, A.D. (1997), "A comparative study of subgrid scale models in homogeneous isotropic turbulence", *Phys. Fluids*, Vol. 9 No. 5, pp. 1416-29.

Galperin, B. and Orszag, S. (1993), *Large Eddy Simulation of Complex Engineering and Geophysical Flows*, Cambridge University Press, Cambridge.

Gosman, A.D., Tsui, Y.Y. and Watkins, A.P. (1984), *Calculation of Three Dimensional Air Motion Model Engines*, SAE 840229.

Ikegami, M., Kidoguchi, Y. and Nishiwaki, K. (1986), *A Multidimensional Model Prediction of Heat Transfer in Non-Fired Engines*, SAE 860467.

Kershaw, D. (1978), "The incomplete Cholesky-conjugate gradient method for the iterative solution of systems of linear equations", *J. Comp. Phys.*, Vol. 26, pp. 43-65.

Kondoh, T., Fukumoto, A., Ohsawa, K. and Ohkubo, Y. (1986), *An Assessment of a Multi-Dimensional Numerical Method to Predict the Flow in Internal Combustion Engines*, SAE 850500.

Lawton, B. (1987), "Effect of compression and expansion on instantaneous heat transfer in reciprocating internal combustion engines", *Proc. Instn. Mech. Engrs.*, Vol. 201 No. A3, pp. 175-85.

Morel, T., Wahiduzzaman, S., Tree, D.R. and Dewitt, D.P. (1987), *Effect of Speed, Load, and Location on Heat Transfer in a Diesel Engine – Measurement and Predictions*, SAE 870154.

Raithby, G. and Van Doormaal, I. (1984), "Enhancements of the SIMPLE method for predicting incompressible fluid flows", *Num. Heat Trans.*, Vol. 7, pp. 147-63.

Smagorinsky, J. (1963), "General circulation experiments with the primitive equations", *Mon. Wea. Rev.*, Vol. 91, March, pp. 99-164.

Smith, J.R. (1996), *An Accurate Navier-Stokes Solver With an Application to Unsteady Flows*, West Virginia University, Morgantown, WV.

Tsui, Y.Y. (1991), "A study of upstream weighted high-order differencing for approximation to flow convection", *Int. J. Numerical Methods in Fluids*, Vol. 13, pp. 167-99.

Tu, J.Y. and Fuchs, L. (1992), "Overlapping grids and multigrid methods for three-dimensional unsteady flow calculation in IC engines", *Int. J. Num. Methods in Fluids*, Vol. 15, pp. 693-714.

Van Der Vorst, H. (1992), "BI-CGSTAB: a fast and smoothly converging variant of BI-CG for the solution of nonsymmetric linear system", *SIAM J. Sci. Stat. Comput.*, Vol. 13 No. 2, pp. 631-44.

Wilcox, D. (1993), *Turbulence Modeling in CFD, DCW Industries*, Inc., Glendale, CA.

Woschni, G. and Fieger, J. (1980), *Determination of Local Heat Transfer Coefficients at the Piston of a High Speed Diesel Engine by Evaluation of Measured Temperature Distribution*, SAE 790834.

Yamada, S., Paulsen, H. and Farrel, P. (1989), *Heat Transfer Measurements in a Motored Engine*, SAE 890313.

Yang, J., Pierce, P., Martin, J.K. and Foster, D.E. (1988), "Heat transfer predictions and experiments in a motored engine", *SAE Trans. 881314*, Vol. 97, Section 6, pp. 1608-22.